● RESEARCH ARTICLE

Protective mechanisms of microRNA-27a against oxygen-glucose deprivation-induced injuries in hippocampal neurons

Qun Cai[1], Ting Wang[2], Wen-jie Yang[3], Xing Fen[1, *]

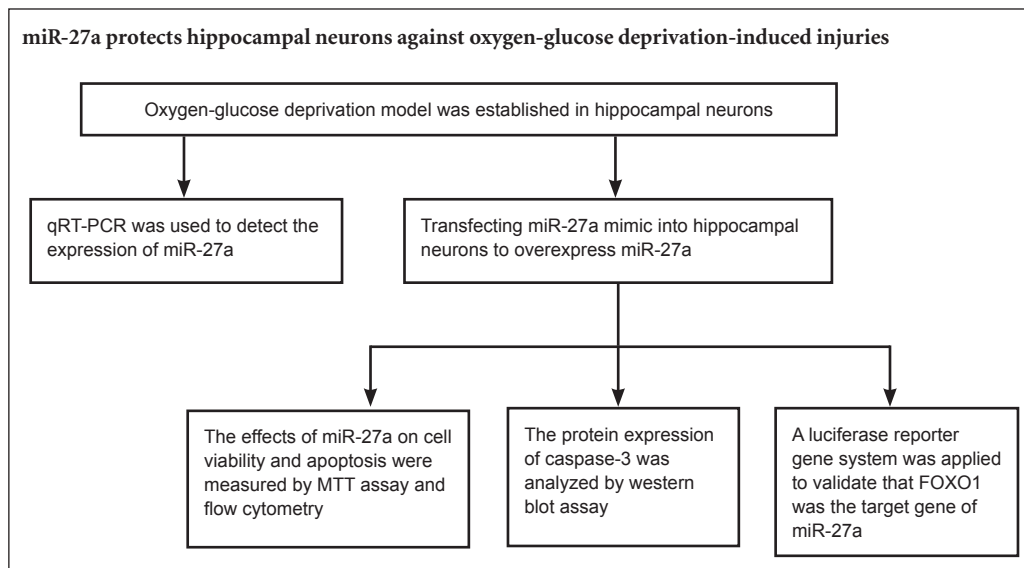1 Department of Neonatology, Children's Hospital of Soochow University, Suzhou, Jiangsu Province, China
2 Department of Emergency, Affiliated Hospital of Nantong University, Nantong, Jiangsu Province, China
3 Medical College of Nantong University, Nantong, Jiangsu Province, China

Graphical Abstract

miR-27a protects hippocampal neurons against oxygen-glucose deprivation-induced injuries

Oxygen-glucose deprivation model was established in hippocampal neurons

qRT-PCR was used to detect the expression of miR-27a

Transfecting miR-27a mimic into hippocampal neurons to overexpress miR-27a

The effects of miR-27a on cell viability and apoptosis were measured by MTT assay and flow cytometry

The protein expression of caspase-3 was analyzed by western blot assay

A luciferase reporter gene system was applied to validate that FOXO1 was the target gene of miR-27a

Correspondence to:
Xing Fen, M.D.,
fenxing@hotmail.com.

orcid:
0000-0002-4540-1348
(Qun Cai)

Abstract

Hypoxic injuries during fetal distress have been shown to cause reduced expression of microRNA-27a (miR-27a), which regulates sensitivity of cortical neurons to apoptosis. We hypothesized that miR-27a overexpression attenuates hypoxia- and ischemia-induced neuronal apoptosis by regulating *FOXO1*, an important transcription factor for regulating the oxidative stress response. miR-27a mimic was transfected into hippocampal neurons to overexpress miR-27a. Results showed increased hippocampal neuronal viability and decreased caspase-3 expression. The luciferase reporter gene system demonstrated that miR-27a directly binded to *FOXO1* 3′UTR in hippocampal neurons and inhibited *FOXO1* expression, suggesting that *FOXO1* was the target gene for miR-27a. These findings confirm that miR-27a protects hippocampal neurons against oxygen-glucose deprivation-induced injuries. The mechanism might be mediated by modulation of *FOXO1* and apoptosis-related gene caspase-3 expression.

Key Words: nerve regeneration; brain injury; miR-27a; hypoxic-ischemic; hippocampal neurons; oxygen-glucose deprivation; cell survival; apoptosis; caspase 3; FOXO1; luciferase reporter gene system; neuroprotection; neural regeneration

Introduction

During the perinatal stage, ischemia and hypoxia are the main causes of infant hypoxic-ischemic brain damage (HIBD), which can lead to mortality and neurological disability in infants and young children and occurs in 1 to 6 of every 1,000 live-term births (Hristova et al., 2015; Yu et al.,

2015; Lai et al., 2016). Fetal distress, hypoxia due to an umbilical cord around the neck, and intrauterine infection can lead to an insufficient oxygen and blood supply for fetal or neonatal brain tissue (Chen et al., 2013; Fitch et al., 2013). Approximately 40% of newborn infants with HIBD die during the neonatal period, and an additional 30% sustain lifelong

neurological deficits, including cerebral palsy, epilepsy, and cognitive disabilities (Charon et al., 2015; Li et al., 2015a). Treatment of HIBD sequelae requires enormous efforts. However, even with the best management, there is often little improvement in the overall ability of these children (Liu et al., 2015a).

The discovery of microRNAs (miRNAs) brings a new understanding of HIBD, and provides novel strategies and targets for HIBD treatment. miRNAs are small, non-coding RNAs that are 17–25 nucleotides in length (Jiang et al., 2016). miRNAs serve as posttranscriptional regulators by binding to the targeting gene mRNA 3′untranslated region (3′UTR), thereby inducing degradation or translation inhibition (Li et al., 2015b; Zhou et al., 2016). An increased understanding of miRNAs brings novel insight into the regulation of gene expression, consequently playing regulatory roles in a wide variety of physiological and pathological cellular processes (Rajasekaran et al., 2015; Katsura et al., 2016).

During myocardial ischemia/reperfusion injury, miR-22 has been shown to play an important cardioprotective role, partly by regulating the CBP/AP-1 pathway to reduce cell apoptosis and inflammatory damage (Yang et al., 2016). Similarly, some miRNAs may be deregulated, thereby influencing pathological changes in the nervous system (Wu and Murashov, 2013; Lechpammer et al., 2015; Looney et al., 2015). Zhang et al. (2012) reported that hypoxia caused increased FasL expression, but decreased miR-21 expression in microglia, suggesting that miR-21 could play an important role in potential novel therapeutic interventions for cerebral hypoxic diseases associated with microglial activation.

Numerous studies have revealed that miR-27a plays an oncogenic role in the development and progression of human cancers (Park et al., 2015; Towers et al., 2015; Zhou et al., 2015b). Chen et al. (2014) reported that hypoxic injuries during fetal distress cause reduced miR-23b and miR-27b expression, which further inhibits Apaf-1 expression and regulates neuronal sensitivity to apoptosis. However, the biological roles of miR-27a in hypoxia and ischemia remain poorly understood.

In the present study, we investigated the expression of miR-27a in oxygen-glucose deprivation (OGD)/reoxygenation-exposed hippocampal neurons to better understand its role in HIBD. We overexpressed miR-27a to analyze the effects of miR-27a on viability and apoptosis of OGD-treated neuronal cells. Results from the present study could provide a better understanding of miR-27a as a potential therapeutic target in the treatment of hypoxic-ischemic encephalopathy.

Materials and Methods
Cell culture
The experimental procedures involving animals were conducted according to the institutional animal care guidelines of Nantong University, China, and were ethically approved by the Administration Committee for Experimental Animals, Jiangsu Province, China.

Isolation and culture of rat hippocampal neurons were accomplished according to previously described methods with minor modifications (Booth et al., 2016).

Rat primary hippocampal neuron cultures were prepared from embryonic day 18 (E18)–E19, specific-pathogen-free, Sprague-Dawley rat (Laboratory Animal Center of Nantong University, China) embryos (SYXK (Su) 2012-0031). In brief, after rats were sacrificed under anesthesia, their brains were quickly removed; the hippocampal tissues were harvested on a cold stage, and dissociated with trypsin-ethylenediamine tetraacetic acid (0.25%) into cell suspensions, which were plated onto poly-lysine-coated plates at a density of 1×10^6/mL. The cells were maintained in serum-free Neurobasal medium (Life Technologies, Carlsbad, CA, USA) with 2% B27 (Gibco, Carlsbad, CA, USA) for 7 days, after which half of the medium was replaced every 3 days. The cells were then subjected to immunohistochemistry for neurofilament protein and fibrillary acidic protein, revealing that cell cultures contained approximately 95% neurons.

Human embryonic kidney 293 (HEK293) cells were obtained from American Type Culture Collection (Manassas, VA, USA) and grown in Dulbecco's-modified Eagle's medium (DMEM, Life Technologies, Carlsbad, CA, USA) containing 10% fetal bovine serum (Gibco). When HEK293 cell growth reached 70% to 80% confluency, the cells were digested with 0.25% trypsin and passaged. The culture medium was replaced every other day, and the cells were passaged every 3 to 4 days. Cells in the logarithmic growth phase were collected for experiments. Cell growth was observed under an inverted microscope, and cells were cultured in an incubator with 5% CO_2 and saturated humidity at 37°C.

OGD/reoxygenation modeling of hippocampal neurons
OGD/reoxygenation model of hippocampal neurons was established in accordance with previously described methods with minor modifications (Gu et al., 2016). In brief, the cells were transferred to glucose-free DMEM bubbled with 95% N_2/5% CO_2 in a sealed humidified modular incubator chamber (MIC-101, Billups-Rothenberg, Del Mar, CA) for 3 hours. For reperfusion, the exposure medium was replaced with neuronal culture medium, and the cells were incubated in a normoxic incubator for an additional 6–24 hours. At the end of cell treatment, the cell cultures were subjected to various assessments. Cells were divided into four groups. In three of the groups, hippocampal neurons were subjected to OGD/reoxygenation treatment for 6, 12, and 24 hours, respectively. In the fourth group, the cells were cultured in plain DMEM and neuronal culture medium with ambient oxygen for 6–24 hours, respectively, which served as the control (no exposure to OGD).

RNA isolation and quantitative real-time polymerase chain reaction (qRT-PCR)
Hippocampal neurons were transfected with mi-27a mimics and mimic control (ctrl) (Ribobio, Guangzhou, Guangdong

Province, China), respectively, using Lipofectamine RNAi-MAX transfection reagent (Invitrogen, Carlsbad, CA, USA) according to manufacture instructions.

Total RNA at 48 hours post-transfection, including miR-NAs, was extracted using the TaqMan miRNA Isolation kit (Applied Biosystems, Foster, CA, USA). NanoDropND-1000 spectrophotometry (NanoDrop Tech, Wilmington, DE, USA) was used to measure RNA concentrations. PCR was then used to amplify miR-27a using SYBR Premix Ex TaqTM II (Perfect Real Time; TaKaRa, Tokyo, Japan) and miR-27a-specific primers. Primer sequences are shown in **Table 1**. All reactions were performed in triplicate. The relative expression of miR-27a was normalized to the internal reference U6. Data were analyzed using the $2^{-\Delta\Delta Ct}$ method (Yu et al., 2012).

Cell viability assay
To measure cell viability, the 3-(4,5-dimethyl-2-thiazolyl)-2,5-diphenyl-2-H-tetrazolium bromide (MTT) assay was performed according to the MTT kit (Sigma-Aldrich, St. Louis, MO, USA) instruction protocol. Briefly, hippocampal neurons were seeded in 96-well plates subjected to OGD/reoxygenation treatment for 6, 12, and 24 hours, respectively. The original media were discarded and fresh medium containing MTT (5 mg/mL) was added prior to incubation for an additional 4 hours. Optical density values were measured by spectrophotometry at 570 nm with an ELX-800 microplate reader (Bio-Tek Inc., Winooski, VT, USA). Three independent assays were conducted.

Cell apoptosis assay
Flow cytometry and Annexin V/propidium iodide (PI) staining were used to analyze cell apoptosis. After 12 hours of treatment (OGD/reoxygenation), cells were harvested and washed once or twice with PBS, followed by addition of Annexin V-fluorescein isothiocyanate (FITC) and PI staining reagents (BioVision, Cliniscience, Montrouge, France). The mixture was incubated in the dark for 15 minutes. After filtration with a screen cloth, the cells were analyzed using flow cytometry (BD Bioscience, San Jose, CA, USA). FITC$^+$/PI$^-$ cells were considered early apoptotic cells. Flow cytometry CellQuest software (BD Bioscience) was used to quantify the cells, and Macquit software was used to analyze the data.

Luciferase reporter assay
The 3′-UTR sequence of *FOXO1* (NM_001191846 in Gen-Bank) was amplified from rat genomic DNA and subcloned into the luciferase gene in the luciferase reporter vector (Promega, Madison, CA, USA) at the restriction enzyme cleavage site. With appropriate primers, PCR amplification of the 3′-UTR sequence of *FOXO1* generated different pGL3-Luciferase reporter vectors. The wildtype and mutant 3′-UTR sequences were confirmed by sequencing. HEK 293 cells were cultured under standard conditions and inoculated into a 96-well plate at 3×10^5 cells/mL (100 μL/well). The *FOXO1* 3′-UTR luciferase plasmid containing the *FOXO1* 3′-UTR, miR-27a mimic, or a negative control was transfected following the recommended protocol for the Lipofectamine 2000 transfection system (Invitrogen, Carlsbad, CA, USA), and a normal control was also included. After 48 hours of incubation, luciferase activities were measured using the luciferase reporter assay system (Promega, Madison, WI, USA) from cell lysates.

Western blot assay
Total proteins after 48 hours of treatment were extracted with a lysis buffer containing protease inhibitors (Promega) from primary neuronal cells and quantified using the Pierce™ Bicinchoninic Acid Protein Assay kit (Pierce Biotechnology, Rockford, IL, USA). Protein (30 μg) was loaded into each lane and electrophoretically separated on a 10% sodium dodecyl sulphate-polyacrylamide gel, and transferred to polyvinylidene fluoride membrane (GE Healthcare, Little Chalfont, UK). The membrane was incubated with 5% (w/v) non-fat milk in Tris-buffered saline with Tween 20 (50 mM Tris-HCl, 100 mM NaCl, and 0.1% Tween-20, pH 7.4) at room temperature for 1 hour. The membranes were incubated with rabbit anti-rat pro-caspase-3 polyclonal antibody and rabbit anti-rat cleaved caspase-3 polyclonal antibody (1:1,000; Cell Signaling, Danvers, MA, USA), rabbit anti-rat FOXO1 polyclonal antibody (1:2,000; Abcam, Cambridge, MA, USA), and anti-rat β-actin monoclonal antibody (1:5,000; Sigma, St Louis, MO, USA), respectively, at 4°C overnight. The membrane was incubated with secondary donkey anti-rabbit horseradish peroxidase conjugated antibodies (1:2,000; Abcam) for 2 hours at room temperature. Immunoreactive proteins were visualized by an enhanced chemiluminescence-plus chemiluminescence reaction. The relative contents of pro-caspase-3, cleaved caspase-3, and FOXO1 were represented as the gray scale ratio of cleaved caspase-3/pro-caspase-3, and FOXO1/β-actin, and the gray scale was analyzed using QuantityOne software (Bio-Rad, Hercules, CA, USA).

Statistical analysis
All data were expressed as mean ± SEM from three independent experiments (each in duplicate). The Student's *t*-test and one-way analysis of variance followed by the *post-hoc* Scheffe's test were used for statistical analysis using the Stata 6.0 software package (Stata Corp., College Station, TX, USA). A value of $P < 0.05$ was considered statistically significant.
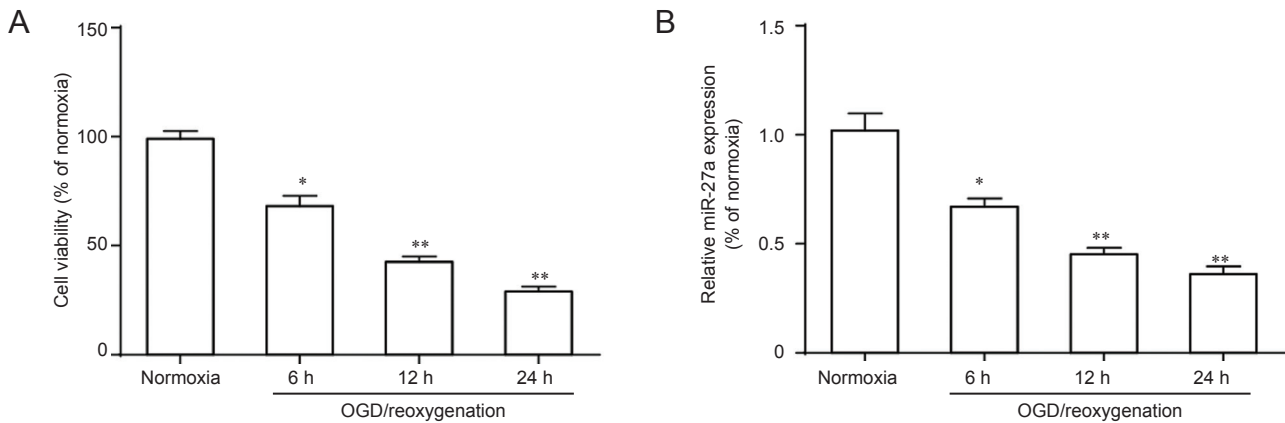
Results
Neuronal cell viability and miR-27a expression in OGD/reoxygenation-treated primary cultured hippocampal neurons
The MTT assay was used to analyze cell viability of hippocampal neurons after cell treatment. Results showed that during 6–24 hours of reoxygenation post-OGD, neuronal cell viability decreased compared with control (normoxia) ($P < 0.05$). Neuronal cell viability exposed to OGD/reoxygenation for 12 and 24 hours was significantly decreased compared with normoxia control ($P < 0.01$) (**Figure 1A**). Thus,

Table 1 Primer sequences for quantitative real-time polymerase chain reaction

Gene		Sequence	Product size (bp)
miR-27a	Forward	5′-ACA CTC CAG CTG GGT TCA CAG TGG CTA AG-3′	20
	Reverse	5′-TGG TGT CGT GGA GTC G-3′	
U6	Forward	5′-CTC GCT TCG GCA GCA CA-3′	94
	Reverse	5′-AAC GCT TCA CGA ATT TGC GT-3′	

Figure 1 Neuronal cell viability and miR-27a expression in OGD-induced primary cultured hippocampal neurons.
(A) MTT assay was used to measure neuronal cell viability. (B) Expression of miR-27a was detected by qRT-PCR, and miR-27a expression was normalized to U6. Histogram shows cell viability or miR-27a expression in primary hippocampal neurons exposed to OGD/reoxygenation for 6, 12, and 24 hours, or normoxia, respectively. *$P < 0.05$, **$P < 0.01$, *vs.* normoxia control (mean ± SEM; experiments were performed in triplicate; one-way analysis of variance followed by *post-hoc* Scheffe's test). MTT: 3-(4,5-Dimethyl-2-thiazolyl)-2,5-diphenyl-2-H-tetrazolium bromide; qRT-PCR: quantitative real-time polymerase chain reaction; OGD: oxygen-glucose deprivation; h: hours.
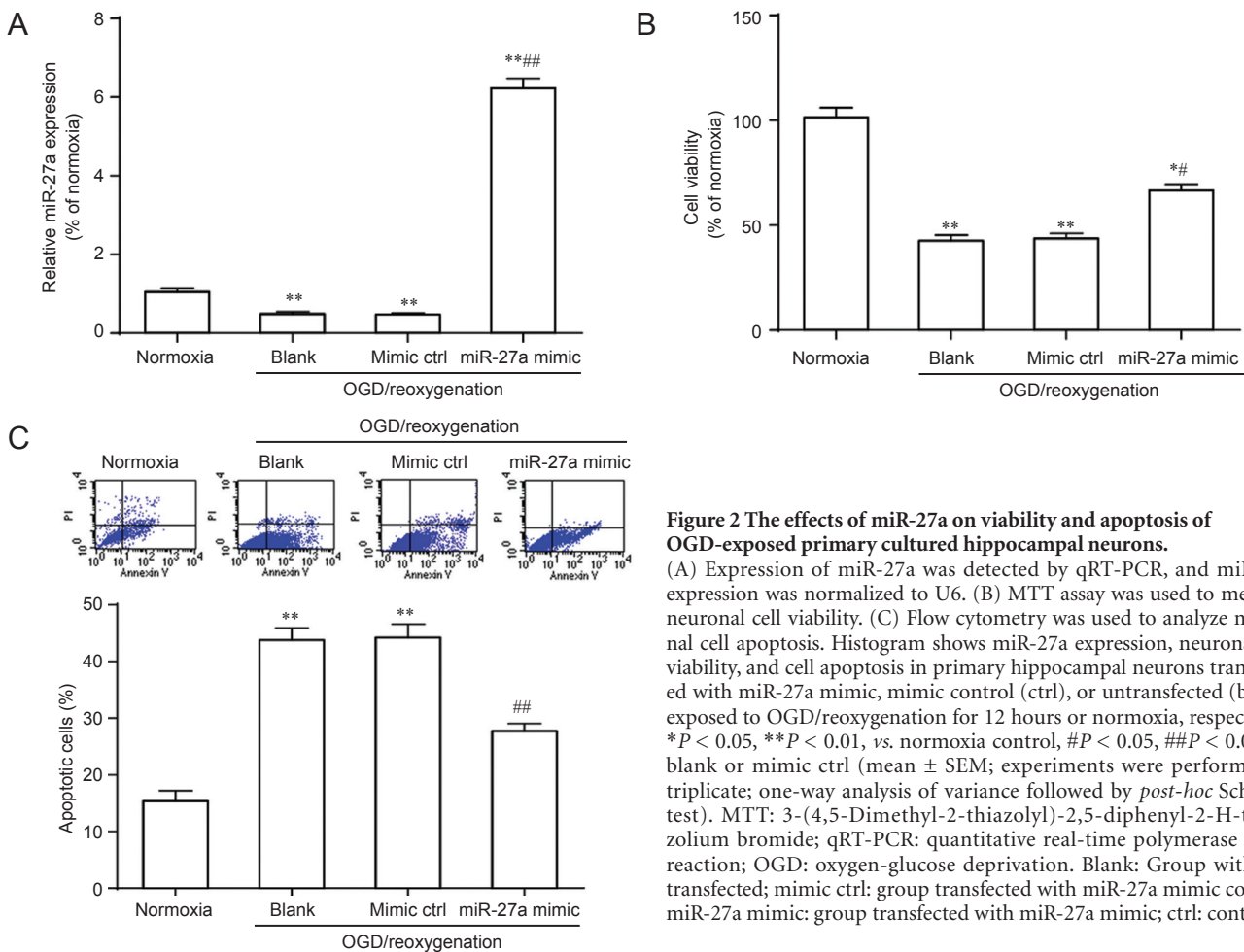
Figure 2 The effects of miR-27a on viability and apoptosis of OGD-exposed primary cultured hippocampal neurons.
(A) Expression of miR-27a was detected by qRT-PCR, and miR-27a expression was normalized to U6. (B) MTT assay was used to measure neuronal cell viability. (C) Flow cytometry was used to analyze neuronal cell apoptosis. Histogram shows miR-27a expression, neuronal cell viability, and cell apoptosis in primary hippocampal neurons transfected with miR-27a mimic, mimic control (ctrl), or untransfected (blank) exposed to OGD/reoxygenation for 12 hours or normoxia, respectively. *$P < 0.05$, **$P < 0.01$, *vs.* normoxia control, #$P < 0.05$, ##$P < 0.01$, *vs.* blank or mimic ctrl (mean ± SEM; experiments were performed in triplicate; one-way analysis of variance followed by *post-hoc* Scheffe's test). MTT: 3-(4,5-Dimethyl-2-thiazolyl)-2,5-diphenyl-2-H-tetrazolium bromide; qRT-PCR: quantitative real-time polymerase chain reaction; OGD: oxygen-glucose deprivation. Blank: Group with untransfected; mimic ctrl: group transfected with miR-27a mimic control; miR-27a mimic: group transfected with miR-27a mimic; ctrl: control.

we chose OGD/reoxygenation for 12 hours in the following experiments. After OGD treatment, primary hippocampal neurons exhibited morphological alterations, such as neurite disappearance and vacuolus emergence around the cell body (data not shown).

To further confirm miR-27a expression in hippocampal neurons following OGD/reoxygenation, we detected miR-27a levels at various times by qRT-PCR. After neurons were induced by OGD/reoxygenation, the relative expression levels of miR-27a gradually decreased compared with control (normoxia) ($P < 0.05$; **Figure 1B**).

Effects of miR-27a on viability and apoptosis of OGD/reoxygenation-treated hippocampal neurons

To investigate whether miR-27a dysregulation was sufficient to impact cell function against OGD-induced injury, hippocampal neurons were transfected with miR-27a mimic and non-targeting negative control (mimic ctrl) before OGD. Expression of miR-27a was detected by qRT-PCR in neurons transfected for 48 hours, showing significantly increased expression (5-fold) in neurons transfected with mimic compared with control (normoxia) ($P < 0.01$; **Figure 2A**).

The MTT assay was used to analyze miR-27a effects on OGD/reoxygenation-treated cell viability. Results showed that miR-27a overexpression promoted cell viability compared with untransfected control (blank) and mimic control (mimic ctrl) ($P < 0.05$; **Figure 2B**).

Flow cytometry was used to test miR-27a effects on OGD/reoxygenation-treated cell apoptosis. As shown in **Figure 2C**, the percentage of apoptotic neurons transfected with miR-27a mimic was significantly less than in the untransfected control (blank) and mimic control (mimic ctrl) ($P < 0.01$).

FOXO1 is a direct target of miR-27a

miRNAs exert their biological functions through suppression of target genes (Yu et al., 2012). Thus, it is necessary to identify the miRNA and gene target pairs. Online software analysis showed that *FOXO1* might serve as the target gene (http://www.targetscan.org/). To verify whether the predicted miR-27a target was located in the *FOXO1* 3′UTR, we constructed a luciferase plasmid containing *FOXO1* 3′UTR and mutated *FOXO1* 3′-UTR, and the plasmid, together with miR-27a mimic and mimic control, was co-transfected into HEK293 cells. Relative luciferase activity was significantly decreased by miR-27a when wildtype *FOXO1* 3′UTR was present (**Figure 3**).

Effect of miR-27a on caspase-3 activation in OGD/reoxygenation-treated primary cultured hippocampal neurons

Western blot assay was applied to analyze pro-caspase-3 and cleaved caspase-3 expression in neurons after OGD/reoxygenation. Cleaved caspase-3 is the active subunit of pro-caspase-3 (Cui et al., 2016). Expression of cleaved caspase-3 significantly increased in neurons treated with OGD/reoxygenation compared with normoxia ($P < 0.01$), while pro-

caspase-3 expression slightly decreased. Additionally, miR-27a inhibited cleaved caspase-3 expression after OGD/reoxygenation compared with untransfected control (blank) and mimic control (ctrl) ($P < 0.05$; **Figure 4**).

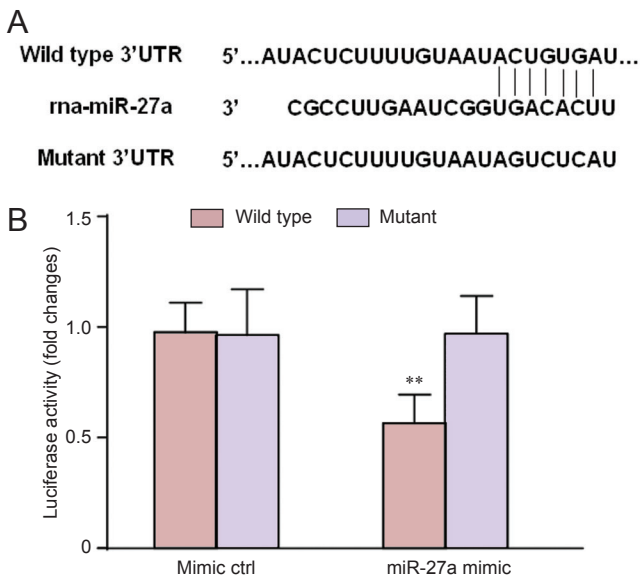### Effect of miR-27a on *FOXO1* expression in neuronal cells

Western blot assay was used to measure *FOXO1* expression in neuronal cells. Results showed significantly reduced *FOXO1* expression in neurons transfected with miR-27a mimic compared with untransfected control (ctrl) and mimic control (ctrl) ($P < 0.01$; **Figure 5**).

Discussion

HIBD is a clinical condition in the neonate, resulting from oxygen deprivation around the time of birth, and a major public health issue globally with long-term effects on the family, health care system, and society (Orrock et al., 2015; Luckman et al., 2016; Xie et al., 2016). The involvement of miRNAs in regulating various cellular processes, including cell proliferation, apoptosis, and differentiation, provides novel insights in disease research, diagnosis, prognosis, and treatment (Yang et al., 2014; Chandrasekaran and Bonchev, 2016; Jeon and Osborne, 2016). Brain protection in neonatal infants remains a challenging priority and represents a medical requirement that has yet to be met (Berger et al., 2015; Lai et al., 2016). In the present study, miR-27a levels measured by qRT-PCR decreased in primary rat hippocampal neurons after OGD/reoxygenation, indicating that miR-27a might be involved in HIBD.

Previous studies have shown that the combined effects of hemodynamic changes, as well as the excitotoxicity impact of excitatory amino acids, nitric oxide, intracellular calcium overloads, and free radical injury, result in neuronal structural damage and apoptosis, eventually leading to neurological functional defects and loss (Chang et al., 2013; Beppu et al., 2014; Du et al., 2014; Ginet et al., 2014; Li et al., 2015c). Although apoptosis occurs after hypoxia and ischemia in both the embryonic and adult stages, a large number of studies have suggested that apoptosis after brain injuries caused by hypoxia and ischemia plays a more prominent role in the neofetus than in the adult (Gao et al., 2015; Jantzie et al., 2015; Xie et al., 2016). Alleviating or reducing neuronal apoptosis in the neofetal brain is key for treating HIBD. In the present study, transfection of miR-27a mimic into hippocampal neurons resulted in miR-27a overexpression, and the effects of miR-27a on cell survival/viability and apoptosis were measured by MTT assay and flow cytometry. Interestingly, we found that upregulated miR-27a promoted cell survival and reduced OGD/reoxygenation-induced neuronal apoptosis, suggesting that miR-27a might play an important role in neuroprotection against OGD by reducing neuronal apoptosis.

Apoptosis involves a series of gene activation, expression, and regulation (Teo et al., 2015; Zhang et al., 2015b). The essential step in the mitochondria-dependent apoptosis pathway is the formation of apoptosomes, consisting of cytochrome c, apoptotic protease activating factor-1, pro-caspase-9, and

A

Wild type 3'UTR 5'...AUACUCUUUUGUAAUACUGUGAU...

rna-miR-27a 3' CGCCUUGAAUCGGUGACACUU

Mutant 3'UTR 5'...AUACUCUUUUGUAAUAGUCUCAU

B

Figure 3 *FOXO1* is a direct target of miR-27a.
(A) Schematic representation of a section of *FOXO1* 3′-UTR showing the putative miR-27a target site. (B) The resulting histogram shows relative luciferase activities in each group. **$P < 0.01$, *vs.* mimic ctrl (mean ± SEM; experiments were performed in triplicate; one-way analysis of variance followed by *post-hoc* Scheffe's test). 3′-UTR: 3′ Untranslated region. Mimic ctrl: Group transfected with miR-27a mimic control; miR-27a mimic: group transfected with miR-27a mimic; ctrl: control.

A

B
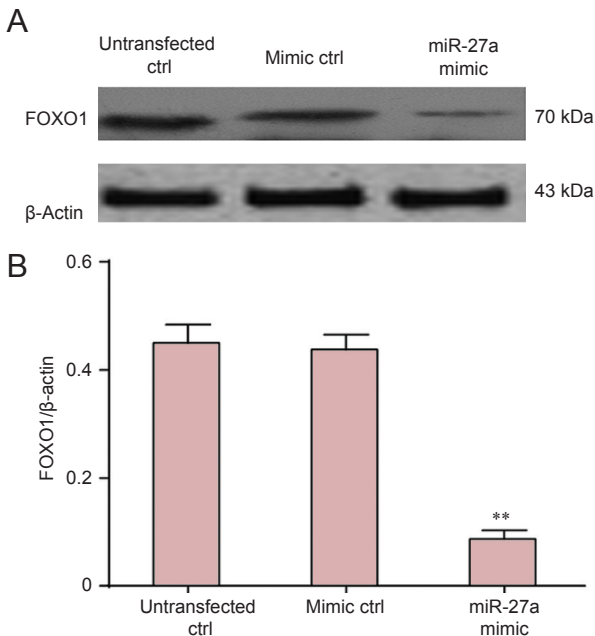
Figure 5 Effect of miR-27a on FOXO1 protein expression in rat primary hippocampal neurons.
Representative western blot image (the upper) and resulting histogram (the lower) show FOXO1 protein expressions in neurons transfected with miR-27a mimic, mimic ctrl, or untransfected, respectively. **$P < 0.01$, *vs.* untransfected ctrl and mimic ctrl (mean ± SEM; experiments were performed in triplicate; Student's *t*-test). Untransfected ctrl: Normal group; Mimic ctrl: group transfected with miR-27a mimic control; miR-27a mimic: group transfected with miR-27a mimic; ctrl: control.

A

B
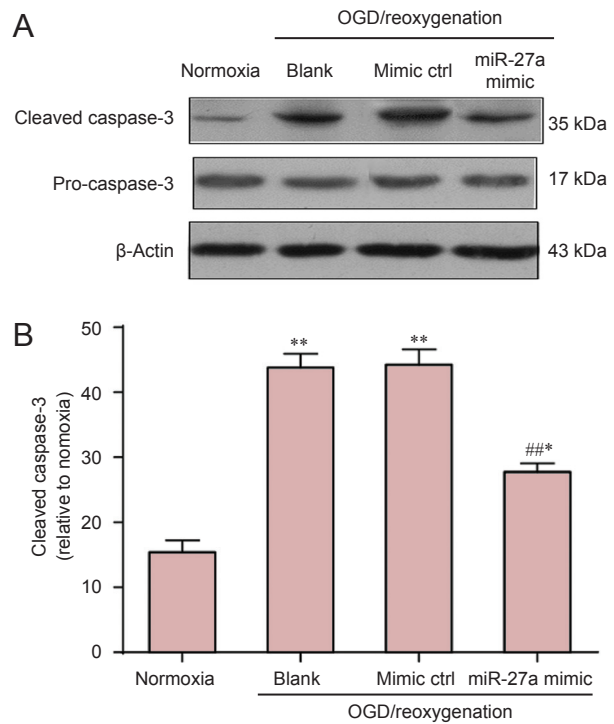
Figure 4 Effect of miR-27a on caspase-3 activation in OGD-exposed primary cultured hippocampal neurons.
Representative western blot image (the upper) and resulting histogram (the lower) show cleaved caspase-3 expression in primary hippocampal neurons transfected with miR-27a mimic, mimic ctrl, or untransfected (blank) after exposure to OGD/reoxygenation for 12 hours or normoxia, respectively. *$P < 0.05$, $P < 0.01$, *vs.* normoxia control; ##$P < 0.01$, *vs.* blank control or mimic ctrl (mean ± SEM; experiments were performed in triplicate; one-way analysis of variance followed by *post-hoc* Scheffe's test). OGD: Oxygen-glucose deprivation; Blank: group with untransfected; Mimic ctrl: group transfected with miR-27a mimic control; miR-27a mimic: group transfected with miR-27a mimic; ctrl: control.

adenosine triphosphate (Monian and Jiang, 2015; Zhang et al., 2015a; Zhou et al., 2015a). miR-27a/b are endogenous inhibitor factors of apoptotic protease activating factor-1 expression and have been shown to regulate sensitivity of neurons to apoptosis (Chen et al., 2014). Hypoxic-ischemic injury also triggers proteolytic processing of pro-caspase-3, resulting in the formation of a 17-kDa subunit of cleaved caspase-3 (active caspase-3) (Hattori et al., 2015; Liu et al., 2015b). In the present study, western blot assay was applied to analyze pro-caspase-3 and cleaved caspase-3 expression in neurons after OGD/reoxygenation. Additionally, miR-27a inhibited cleaved caspase-3 expression in neurons after OGD/reoxygenation, while pro-caspase-3 expression slightly decreased.

FOXO1 is an important transcription factor for regulating the oxidative stress response, cell proliferation, and apoptosis, and is widely expressed in multiple organs, such as the liver, fat, and skeletal muscle (Kinoshita et al., 2016; Luo et al., 2016). Zhao et al. (2015) indicated that propofol might exert its antioxidative effect through *FOXO1* in H9c2 cells. Our online software results showed that *FOXO1*

might be a target gene for miR-27a. A fluorescence reporter gene system was used to verify the location of the predicted miR-27a target in the *FOXO1* 3′UTR. Relative luciferase activity was significantly decreased by miR-27a when wildtype *FOXO1* 3′UTR was present. This reduction was sequence-specific, because the relative luciferase activity did not decline as sharply in UTRs that contained a mutant binding site compared with a wildtype binding site. Western blot assay revealed that miR-27a significantly reduced *FOXO1* expression.

In conclusion, miR-27a might play an important role in neuroprotection against OGD/reoxygenation by modulation of apoptosis-related gene caspase-3 expression and *FOXO1*. The neuroprotective effect of miR-27a suggests a possible use in the treatment of HIBD in the future.

Author contributions: *XF designed the study. QC, TW, and WJY performed the experiments. QC analyzed data and wrote the paper. All authors approved the final version of the paper.*
Conflicts of interest: *None declared.*
Plagiarism check: *This paper was screened twice using Cross-Check to verify originality before publication.*
Peer review: *This paper was double-blinded and stringently reviewed by international expert reviewers.*

References

Beppu K, Sasaki T, Tanaka KF, Yamanaka A, Fukazawa Y, Shigemoto R, Matsui K (2014) Optogenetic countering of glial acidosis suppresses glial glutamate release and ischemic brain damage. Neuron 81:314-320.

Berger HR, Morken TS, Vettukattil R, Brubakk AM, Sonnewald U, Wideroe M (2016) No improvement of neuronal metabolism in the reperfusion phase with melatonin treatment after hypoxic-ischemic brain injury in the neonatal rat. J Neurochem 136: 339-350.

Booth CA, Witton J, Nowacki J, Tsaneva-Atanasova K, Jones MW, Randall AD, Brown JT (2016) Altered intrinsic pyramidal neuron properties and pathway-specific synaptic dysfunction underlie aberrant hippocampal network function in a mouse model of tauopathy. J Neurosci 36:350-363.

Chandrasekaran S, Bonchev D (2016) Network topology analysis of post-mortem brain microarrays identifies more alzheimer's related genes and micrornas and points to novel routes for fighting with the disease. PLoS One 11:e0144052.

Chang KH, Yeh CM, Yeh CY, Huang CC, Hsu KS (2013) Neonatal dexamethasone treatment exacerbates hypoxic-ischemic brain injury. Mol Brain 6:18.

Charon V, Proisy M, Ferre JC, Bruneau B, Treguier C, Beuchee A, Chauvel J, Rozel C (2015) Comparison of early and late MRI in neonatal hypoxic-ischemic encephalopathy using three assessment methods. Pediatr Radiol 45:1988-2000.

Chen A, Xiong LJ, Tong Y, Mao M (2013) The neuroprotective roles of BDNF in hypoxic ischemic brain injury. Biomed Rep 1:167-176.

Chen Q, Xu J, Li L, Li H, Mao S, Zhang F, Zen K, Zhang CY, Zhang Q (2014) MicroRNA-23a/b and microRNA-27a/b suppress Apaf-1 protein and alleviate hypoxia-induced neuronal apoptosis. Cell Death Dis 5:e1132.

Cui C, Cui N, Wang P, Song S, Liang H, Ji A (2016) Neuroprotective effect of sulfated polysaccharide isolated from sea cucumber stichopus japonicus on 6-OHDA-induced death in sh-sy5y through inhibition of mapk and nf-kappab and activation of PI3K/Akt signaling pathways. Biochem Biophys Res Commun 470:375-383.

Du G, Tu H, Li X, Pei A, Chen J, Miao Z, Li J, Wang C, Xie H, Xu X, Zhao H (2014) Daphnetin, a natural coumarin derivative, provides the neuroprotection against glutamate-induced toxicity in HT22 cells and ischemic brain injury. Neurochem Res 39:269-275.

Fitch RH, Alexander ML, Threlkeld SW (2013) Early neural disruption and auditory processing outcomes in rodent models: implications for developmental language disability. Front Syst Neurosci 7:58.

Gao S, Mo J, Chen L, Wang Y, Mao X, Shi Y, Zhang X, Yu R, Zhou X (2016) Astrocyte GGTI-mediated Rac1 prenylation upregulates NF-kappaB expression and promotes neuronal apoptosis following hypoxia/ischemia. Neuropharmacology 103:44-56.

Ginet V, Spiehlmann A, Rummel C, Rudinskiy N, Grishchuk Y, Luthi-Carter R, Clarke PG, Truttmann AC, Puyal J (2014) Involvement of autophagy in hypoxic-excitotoxic neuronal death. Autophagy 10:846-860.

Gu Y, He M, Zhou X, Liu J, Hou N, Bin T, Zhang Y, Li T, Chen J (2016) Endogenous IL-6 of mesenchymal stem cell improves behavioral outcome of hypoxic-ischemic brain damage neonatal rats by supressing apoptosis in astrocyte. Sci Rep 6:18587.

Hattori T, Sato Y, Kondo T, Ichinohashi Y, Sugiyama Y, Yamamoto M, Kotani T, Hirata H, Hirakawa A, Suzuki S, Tsuji M, Ikeda T, Nakanishi K, Kojima S, Blomgren K, Hayakawa M (2015) Administration of umbilical cord blood cells transiently decreased hypoxic-ischemic brain injury in neonatal rats. Dev Neurosci 37:95-104.

Hristova M, Rocha-Ferreira E, Fontana X, Thei L, Buckle R, Christou M, Hompoonsup S, Gostelow N, Raivich G, Peebles D (2016) Inhibition of signal transducer and activator of transcription 3 (STAT3) reduces neonatal hypoxic-ischemic brain damage. J Neurochem 136:981-994.

Jantzie LL, Winer JL, Corbett CJ, Robinson S (2016) Erythropoietin modulates cerebral and serum degradation products from excess calpain activation following prenatal hypoxia-ischemia. Dev Neurosci 38:15-26.

Jeon TI, Osborne TF (2016) miRNA and cholesterol homeostasis. Biochim Biophys Acta doi:10.1016/j.bbalip.2016.01.005.

Jiang L, Yu L, Zhang X, Lei F, Wang L, Liu X, Wu S, Zhu J, Wu G, Cao L, Liu A, Song L, Li J (2016) miR-892b silencing activates NF-kappaB and promotes aggressiveness in breast cancer. Cancer Res 76:1101-1111.

Katsura A, Suzuki HI, Ueno T, Mihira H, Yamazaki T, Yasuda T, Watabe T, Mano H, Yamada Y, Miyazono K (2016) MicroRNA-31 is a positive modulator of endothelial-mesenchymal transition and associated secretory phenotype induced by TGF-beta. Genes Cells 21:99-116.

Kinoshita A, Locher L, Tienken R, Meyer U, Danicke S, Rehage J, Huber K (2016) Associations between Forkhead Box O1 (FoxO1) Expression and indicators of hepatic glucose production in transition dairy cows supplemented with dietary nicotinic acid. PLoS One 11:e0146670.

Lai Z, Zhang L, Su J, Cai D, Xu Q (2016) Sevoflurane postconditioning improves long-term learning and memory of neonatal hypoxia-ischemia brain damage rats via the PI3K/Akt-mPTP pathway. Brain Res 1630:25-37.

Lechpammer M, Wintermark P, Merry KM, Jackson MC, Jantzie LL, Jensen FE (2016) Dysregulation of FMRP/mTOR signaling cascade in hypoxic-ischemic injury of premature human brain. J Child Neurol 31:426-432.

Li D, Li X, Wu J, Li J, Zhang L, Xiong T, Tang J, Qu Y, Mu D (2015a) Involvement of the JNK/FOXO3a/Bim pathway in neuronal apoptosis after hypoxic-ischemic brain damage in neonatal rats. PLoS One 10:e0132998.

Li Y, Zhao L, Shi B, Ma S, Xu Z, Ge Y, Liu Y, Zheng D, Shi J (2015b) Functions of miR-146a and miR-222 in tumor-associated macrophages in breast cancer. Sci Rep 5:18648.

Li YB, Wang Y, Tang JP, Chen D, Wang SL (2015c) Neuroprotective effects of ginsenoside Rg1-induced neural stem cell transplantation on hypoxic-ischemic encephalopathy. Neural Regen Res 10:753-759.

Liu H, Li W, Rose ME, Hickey RW, Chen J, Uechi GT, Balasubramani M, Day BW, Patel KV, Graham SH (2015) The point mutation UCH-L1 C152A protects primary neurons against cyclopentenone prostaglandin-induced cytotoxicity: implications for post-ischemic neuronal injury. Cell Death Dis 6:e1966.

Looney AM, Walsh BH, Moloney G, Grenham S, Fagan A, O'Keeffe GW, Clarke G, Cryan JF, Dinan TG, Boylan GB, Murray DM (2015) Downregulation of umbilical cord blood levels of mir-374a in neonatal hypoxic ischemic encephalopathy. J Pediatr 167:269-273.

Luckman J, Zahavi A, Efrati S, Gilad G, Snir M, Michowiz S, Goldenberg-Cohen N (2016) Difficulty in distinguishing posterior reversible encephalopathy syndrome, hypoxic-ischemic insult, and acute toxic leukoencephalopathy in children. Neuropediatrics 47:33-38.

Luo CT, Liao W, Dadi S, Toure A, Li MO (2016) Graded Foxo1 activity in T cells differentiates tumour immunity from spontaneous autoimmunity. Nature 529:532-536.

Monian P, Jiang X (2016) The cellular apoptosis susceptibility protein (CAS) promotes TRAIL-induced apoptosis and cell proliferation. J Biol Chem 291:2379-2388.

Orrock JE, Panchapakesan K, Vezina G, Chang T, Harris K, Wang Y, Knoblach S, Massaro AN (2015) Association of brain injury and neonatal cytokine response during therapeutic hypothermia (TH) in newborns with hypoxic-ischemic encephalopathy (HIE). Pediatr Res 79:742-747.

Park JL, Kim M, Song KS, Kim SY, Kim YS (2015) Cell-free mir-27a, a potential diagnostic and prognostic biomarker for gastric cancer. Genomics Inform 13:70-75.

Rajasekaran S, Rajaguru P, Sudhakar Gandhi PS (2015) MicroRNAs as potential targets for progressive pulmonary fibrosis. Front Pharmacol 6:254.

Teo JD, Morris MJ, Jones NM (2015) Hypoxic postconditioning reduces microglial activation, astrocyte and caspase activity, and inflammatory markers after hypoxia-ischemia in the neonatal rat brain. Pediatr Res 77:757-764.

Towers CG, Guarnieri AL, Micalizzi DS, Harrell JC, Gillen AE, Kim J, Wang CA, Oliphant MU, Drasin DJ, Guney MA, Kabos P, Sartorius CA, Tan AC, Perou CM, Espinosa JM, Ford HL (2015) The Six1 oncoprotein downregulates p53 via concomitant regulation of RPL26 and microRNA-27a-3p. Nat Commun 6:10077.

Wang B, Armstrong JS, Reyes M, Kulikowicz E, Lee JH, Spicer D, Bhalala U, Yang ZJ, Koehler RC, Martin LJ, Lee JK (2015) White matter apoptosis is increased by delayed hypothermia and rewarming in a neonatal piglet model of hypoxic ischemic encephalopathy. Neuroscience 316:296-310.

Wu D, Murashov AK (2013) Molecular mechanisms of peripheral nerve regeneration: emerging roles of microRNAs. Front Physiol 4:55.

Xie C, Ginet V, Sun Y, Koike M, Zhou K, Li T, Li H, Li Q, Wang X, Uchiyama Y, Truttmann AC, Kroemer G, Puyal J, Blomgren K, Zhu C (2016) Neuroprotection by selective neuronal deletion of Atg7 in neonatal brain injury. Autophagy 12:410-423.

Yang J, Chen L, Ding J, Zhang J, Fan Z, Yang C, Yu Q, Yang J (2016) Cardioprotective effect of miRNA-22 on hypoxia/reoxygenation induced cardiomyocyte injury in neonatal rats. Gene 579:17-22.

Yang L, Cui H, Cao T (2014) Negative regulation of miRNA-9 on oligodendrocyte lineage gene 1 during hypoxic-ischemic brain damage. Neural Regen Res 9:513-518.

Yu B, Zhou S, Wang Y, Qian T, Ding G, Ding F, Gu X (2012) miR-221 and miR-222 promote Schwann cell proliferation and migration by targeting LASS2 after sciatic nerve injury. J Cell Sci 125:2675-2683.

Zhang L, Dong LY, Li YJ, Hong Z, Wei WS (2012) miR-21 represses FasL in microglia and protects against microglia-mediated neuronal cell death following hypoxia/ischemia. Glia 60:1888-1895.

Zhang L, Chen S, Ruan J, Wu J, Tong AB, Yin Q, Li Y, David L, Lu A, Wang WL, Marks C, Ouyang Q, Zhang X, Mao Y, Wu H (2015a) Cryo-EM structure of the activated NAIP2-NLRC4 inflammasome reveals nucleated polymerization. Science 350:404-409.

Zhang Y, Lan R, Wang J, Li XY, Zhu DN, Ma YZ, Wu JT, Liu ZH (2015b) Acupuncture reduced apoptosis and up-regulated BDNF and GDNF expression in hippocampus following hypoxia-ischemia in neonatal rats. J Ethnopharmacol 172:124-132.

Zhao D, Li Q, Huang Q, Li X, Yin M, Wang Z, Hong J (2015) Cardioprotective effect of propofol against oxygen glucose deprivation and reperfusion injury in H9c2 cells. Oxid Med Cell Longev 2015:184938.

Zhou K, Nguyen LH, Miller JB, Yan Y, Kos P, Xiong H, Li L, Hao J, Minnig JT, Zhu H, Siegwart DJ (2016) Modular degradable dendrimers enable small RNAs to extend survival in an aggressive liver cancer model. Proc Natl Acad Sci U S A 113:520-525.

Zhou M, Li Y, Hu Q, Bai XC, Huang W, Yan C, Scheres SH, Shi Y (2015a) Atomic structure of the apoptosome: mechanism of cytochrome c- and dATP-mediated activation of Apaf-1. Genes Dev 29:2349-2361.

Zhou S, Huang Q, Zheng S, Lin K, You J, Zhang X (2015b) miR-27a regulates the sensitivity of breast cancer cells to cisplatin treatment via BAK-SMAC/DIABLO-XIAP axis. Tumor biol 37:6837-6845.